The Journal of Physical Chemistry Letters

Subscriber access provided by University of Newcastle, Australia

Letter

# Structural Elucidation of cis/trans Dicaffeoylquinic Acid Photoisomerization Using Ion Mobility Spectrometry-Mass Spectrometry

Xueyun Zheng, Ryan S. Renslow, Mpho M Makola, Ian K Webb, Liulin Deng, Dennis G. Thomas, Niranjan Govind, Yehia M. Ibrahim, Mwadham M. Kabanda, Ian Augustus Dubery, Heino Martin Heyman, Richard D. Smith, Ntakadzeni E. Madala, and Erin Shammel Baker

*J. Phys. Chem. Lett.*, **Just Accepted Manuscript** • DOI: 10.1021/acs.jpclett.6b03015 • Publication Date (Web): 07 Mar 2017

**Downloaded from http://pubs.acs.org on March 8, 2017**

**Just Accepted**

"Just Accepted" manuscripts have been peer-reviewed and accepted for publication. They are posted online prior to technical editing, formatting for publication and author proofing. The American Chemical Society provides "Just Accepted" as a free service to the research community to expedite the dissemination of scientific material as soon as possible after acceptance. "Just Accepted" manuscripts appear in full in PDF format accompanied by an HTML abstract. "Just Accepted" manuscripts have been fully peer reviewed, but should not be considered the official version of record. They are accessible to all readers and citable by the Digital Object Identifier (DOI®). "Just Accepted" is an optional service offered to authors. Therefore, the "Just Accepted" Web site may not include all articles that will be published in the journal. After a manuscript is technically edited and formatted, it will be removed from the "Just Accepted" Web site and published as an ASAP article. Note that technical editing may introduce minor changes to the manuscript text and/or graphics which could affect content, and all legal disclaimers and ethical guidelines that apply to the journal pertain. ACS cannot be held responsible for errors or consequences arising from the use of information contained in these "Just Accepted" manuscripts.

ACS Publications

The Journal of Physical Chemistry Letters is published by the American Chemical Society. 1155 Sixteenth Street N.W., Washington, DC 20036
Published by American Chemical Society. Copyright © American Chemical Society. However, no copyright claim is made to original U.S. Government works, or works produced by employees of any Commonwealth realm Crown government in the course of their duties.

# Structural Elucidation of *cis/trans* Dicaffeoylquinic Acid Photoisomerization Using Ion Mobility Spectrometry-Mass Spectrometry

Xueyun Zheng[1‡], Ryan S. Renslow[1‡], Mpho M. Makola[2], Ian K. Webb[1], Liulin Deng[1], Dennis G. Thomas[1], Niranjan Govind[1], Yehia M. Ibrahim[1], Mwadham M. Kabanda[3,4], Ian A. Dubery[2], Heino M. Heyman[1], Richard D. Smith[1], Ntakadzeni E. Madala[2]*, Erin S. Baker[1]*

[1] Earth and Biological Sciences Directorate, Pacific Northwest National Laboratory, Richland, WA 99354, United States

[2] Department of Biochemistry, University of Johannesburg, P.O. Box 524, Auckland Park 2006, South Africa

[3]Department of Chemistry, Faculty of Agriculture, Science and Technology and [4]Material Science Innovation and Modelling (MaSIM) Research Focus Area, School of Mathematical and Physical Science, North-West University, Mafikeng Campus, Private Bag X 2046, Mmabatho 2735, South Africa

[‡] These authors contributed equally.

*Corresponding authors: Erin S. Baker
Address: 902 Battelle Blvd.
P.O. Box 999, MSIN K8-98
Richland, WA 99352
Phone: 509-371-6219
Email: erin.baker@pnnl.gov

Ntakadzeni E. Madala
Address: P.O. Box 524
Auckland Park, 2006
Phone: +27115594573
Email: emadala@uj.ac.za

**Abstract:**

Due to the recently uncovered health benefits and anti-HIV activities of dicaffeoylquinic acids (diCQAs), understanding their structures and functions is of great interest for drug discovery efforts. DiCQAs are analytically challenging to identify and quantify since they commonly exist as a diverse mixture of positional and geometric (*cis/trans*) isomers. In this work, we utilized ion mobility spectrometry coupled with mass spectrometry to separate the various isomers before and after UV irradiation. The experimental collision cross sections were then compared with theoretical structures to differentiate and identify the diCQA isomers. Our analyses found that the diCQAs naturally existed predominantly as *trans/trans* isomers, but after three hours of UV irradiation, *cis/cis*, *cis/trans*, *trans/cis*, and *trans/trans* isomers were all present in the mixture. This is the first report of successful differentiation of *cis/trans* diCQA isomers individually, which shows the great promise of IMS coupled with theoretical calculations for determining the structure and activity relationships of different isomers in drug discovery studies.

# Table of Contents

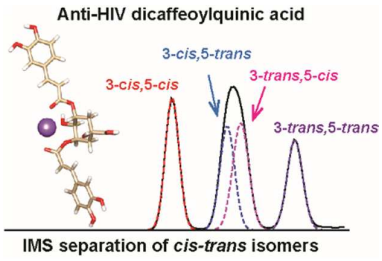




ACS Paragon Plus Environment

Chlorogenic acids (CGAs) are polyphenolic natural products consisting of esters of quinic acid and hydroxycinnamic acids (such as caffeic-, ferulic-, sinapic- or coumaric acid), and found in a wide variety of food and beverage plants. CGAs have been linked to reducing obesity and influenza, and preventing cataractogenesis [1-3], and thus are of great interest for drug discovery efforts. Further, caffeoylquinic acids (CQAs) and dicaffeoylquinic acids (diCQAs), which are the major class of CGAs, also are reported to have antioxidant, anti-HIV, anti-hypertensive, and anti-inflammatory health benefits [4-11]. CGAs, however, normally exist as complex mixtures with various positional and geometric (*cis/trans*) isomers [12-13]. Additionally, exposure to UV light has shown to change the *trans* double bond orientations to *cis*, and when multiple double bonds exist, *cis/cis* and combinations of *cis/trans* isomers are very common [14]. To date, the structure and activity relationship for these *cis*/*trans* isomers has not been well understood, but it is known that the bioactivities of CGAs are affected by the *cis*/*trans* isomerism [15-16].

As mentioned, diCQAs exhibit anti-HIV-1 activity by binding irreversibly to the HIV-1 DNA integrase (a key enzyme for viral HIV DNA integration) and inhibiting HIV-1 DNA replication[7-9]. Related hydroxycinnamic acid derivatives such as L-chicoric acid (dicaffeoyltartaric acid) also possess the same anti-HIV activities, but both the diCQAs and dicaffeoyltartaric acids activities are highly dependent on the structural isomers present [16-18]. Structural isomerization analyses for other natural or synthetic drugs have also shown either agonistic or antagonistic effects. For example, an isomeric mixture of conjugated linoleic acids has been shown to possess enhanced biological activities when compared to the pure components [19], indicating biological synergism of the isomers. Also the unnatural *cis* isomers of potent proteasome inhibitors have exhibited stronger inhibitory activity than the *trans* counterparts [20]. Thus understanding the structures and activities of CGAs is essential for their use in drug studies.

The identification and quantification of phytochemicals in plant extracts is challenging due to their structural diversity, therefore reliable analytical methods capable of differentiating related structures are needed [21]. Although great efforts have been put forth, commonly used analytical platforms have shown significant deficiencies with these separations. For instance, LC-$MS^n$ approaches developed to discriminate positional isomers of CGAs provide limited differentiation of geometric isomers [22-23]. Geometric CGA isomers in previous studies were determined through chromatographic elution orders; however this can be problematic depending on the chromatographic parameters and their reproducibility [14]. Recently it has been reported that *cis* geometrical isomers of diCQAs preferentially bind to alkali metal ions and could be discriminated from the *trans* isomers using LC-MS [24]. However, this method is capable of discriminating the group of *cis* isomers from the group of *trans* isomers, but not identifying individual isomers.

With recent technology advancements, ion mobility spectrometry-mass spectrometry (IMS-MS) has become an appealing tool for the separation and structural characterization of biomolecules [25-26]. IMS-MS has also been used in the characterization of positional and geometrical isomers for small molecules [27-28] and those due to photoisomerization [29-30]. Recently, IMS was applied to separate mono- and diCQAs and differentiate their positional isomers [31-32], but unfortunately the *cis/trans* isomers were not separated. Here we utilized drift tube ion mobility spectrometry-mass spectrometry (DTIMS-MS) to elucidate the *cis*/*trans* isomer structures of diCQAs generated by UV irradiation-induced photoisomerization. Furthermore, a newly developed structures for lossless ion manipulations platform was utilized for ultrahigh resolution IMS separations of the *cis/trans* isomers. SLIM IMS uses traveling waves and a compact serpentine drift path for high ion mobility resolution. A switch can also be utilized in these devices to perform multiple passes in the drift path for even higher IMS resolution[33-38]. The work detailed in this manuscript allowed



ACS Paragon Plus Environment

the structure for each *cis*/*trans* isomer to be unambiguously identified by comparing the experimental collision cross section (CCS) values with theoretical CCS values obtained from molecular modelling. This comparison enabled the differentiation and identification of isomers for these complex natural bioactive phytochemicals, and important for understanding their bioactivity.

In this study, first we characterized the positional isomers for the five diCQA standards (1,3-diCQA, 1,5-diCQA, 3,4-diCQA, 3,5-diCQA, and 4,5-diCQA; Figure 1A) using a 90-cm DTIMS-MS platform (Agilent 6560 IMS-QTOF MS, Santa Clara, California, USA) [39-40]. The DTIMS profiles for these diCQA isomers ($[M+Na]^+$, m/z = 539.12) are shown in Figure 1B. Prior to UV irradiation, each diCQA isomer displayed a single IMS peak, consistent with the fact that these compounds naturally exist as *trans/trans* isomers. The arrival time distributions (ATDs) for these positional isomers were similar; however, 4,5-diCQA eluted first (indicating a smaller structure) and was baseline separated while 1,5-diCQA had the longest arrival time and the largest structure. The CCS value for each diCQA isomer was measured by DTIMS and is given in Table 1. To better differentiate the positional isomers, the SLIM IMS-MS platform was then used to obtain ultrahigh resolution IMS separations. As shown in Figure 1C, after 5 passes of the SLIM IMS-MS platform (67.5 m drift length) 4,5-diCQA, 3,4-diCQA and 1,5-diCQA were well separated, and 1,3-diCQA and 3,5-diCQA partially separated. Since the SLIM IMS-MS platform is based upon traveling waves, direct CCS measurement is not possible without calibration, so only the CCS values from DTIMS are noted in Table 1.

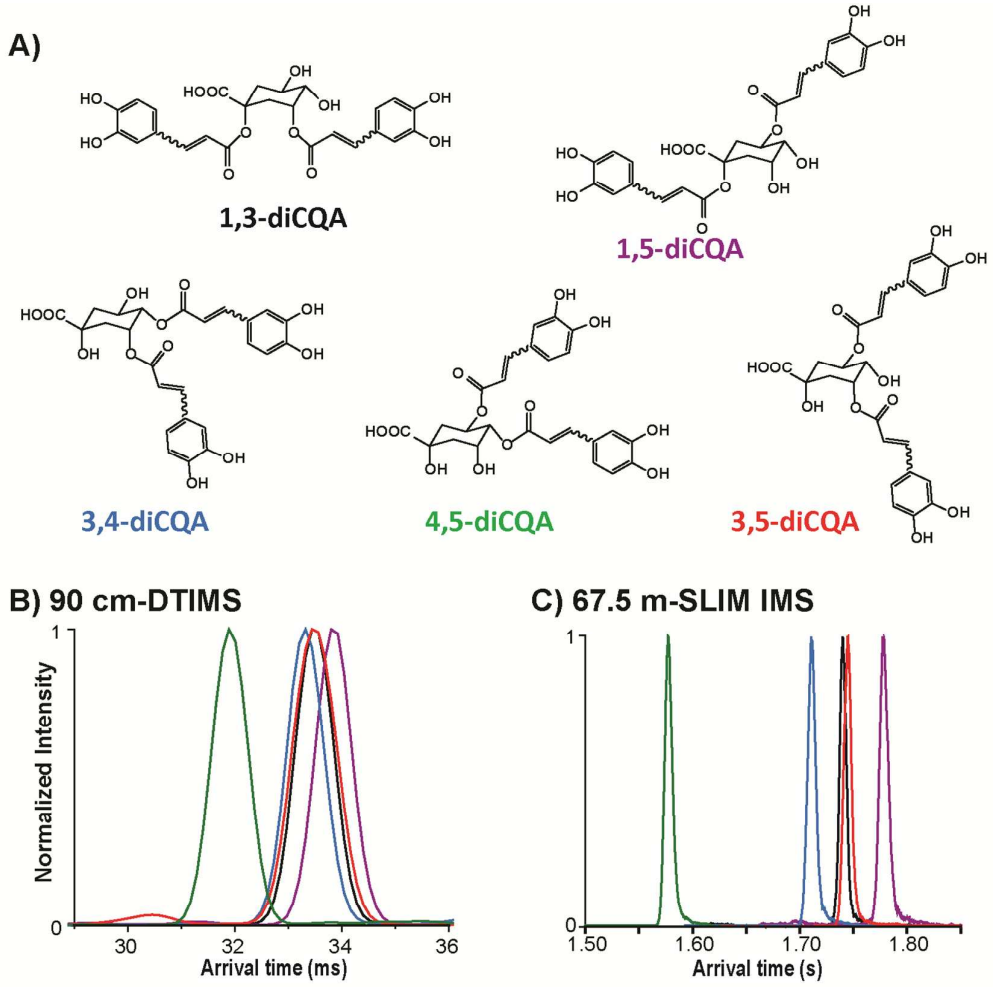


**Figure 1.** IMS characterization of the dicaffeoylquinic acid positional isomers 1,3-diCQA, 1,5-diCQA, 3,4-diCQA, 3,5-diCQA and 4,5-diCQA. **A**) The chemical structures of each isomer and arrival time distributions (ATDs) using a **B**) DTIMS platform and **C**) ultrahigh resolution SLIM IMS.

**Table 1. Experimental collision cross sections measured by DTIMS in nitrogen gas ($^{DT}CCS_{N2}$, in Å$^2$) for each diCQA positional isomer. The coefficient of variance (CV) determined by triplicate measurements were provided.**

| | Experimental $^{DT}CCS_{N2}$ (Å$^2$) | Experimental CV (%) |
|---|---|---|
| 1,3-diCQA | 250 | 0.5 |
| 1,5-diCQA | 252 | 0.3 |
| 3,4-diCQA | 249 | 0.1 |
| 3,5-diCQA | 251 | 0.5 |
| 4,5-diCQA | 236 | 0.1 |

Among these positional isomers, the most abundant form and potent HIV-1 inhibitor 3,5-diCQA was selected to establish an analytical method for *cis*/*trans* isomer separation since four possible geometric isomers exist: 3-*trans*,5-*trans*-diCQA isomer, 3-*cis*,5-*trans*-diCQA, 3-*trans*,5-*cis*-diCQA and 3-*cis*,5-*cis*-diCQA. Previous molecular docking studies showed that these isomers have different binding activities with the HIV-1 INT enzyme, a key enzyme for viral HIV DNA integration [41]. While these isomers all bind to the catalytic domain of HIV-1 INT enzyme, the *cis* isomers were found to bind to the metal cofactor of HIV-1 INT, which is related to its antiviral activity. Moreover, 3-*trans*,5-*cis*-diCQA interacted with both the LYS156 and LYS159 residues that are significant for viral DNA integration. These docking results also showed that different binding activities between the 3,5-diCQA isomers with HIV-1 INT enzyme are synergistic and provide wider inhibition activity than a single isomer. Therefore, understanding the structures of the geometric isomers is important for elucidating their bioactivities.

Upon UV irradiation at 245 nm for 3 hours, the photoisomerization products of 3,5-diCQA were examined by DTIMS-MS (Figure 2). Without UV irradiation, 3,5-diCQA shows mainly a single feature which corresponds to the 3-*trans*,5-*trans* isomer (Figure 2A). An additional peak at a shorter arrival time however was also observed, indicating a small fraction of 3,5-diCQA exists in other conformations prior to UV irradiation. After three hours of UV irradiation, several additional features arose with shorter arrival times (Figure 2B). The feature with the shortest arrival time (left) displayed a very narrow distribution similar to the feature with the longest arrival time (right). The middle feature however was twice as broad as the other features and could be fitted with two features, indicating the presence of two conformations with similar abundances.



ACS Paragon Plus Environment

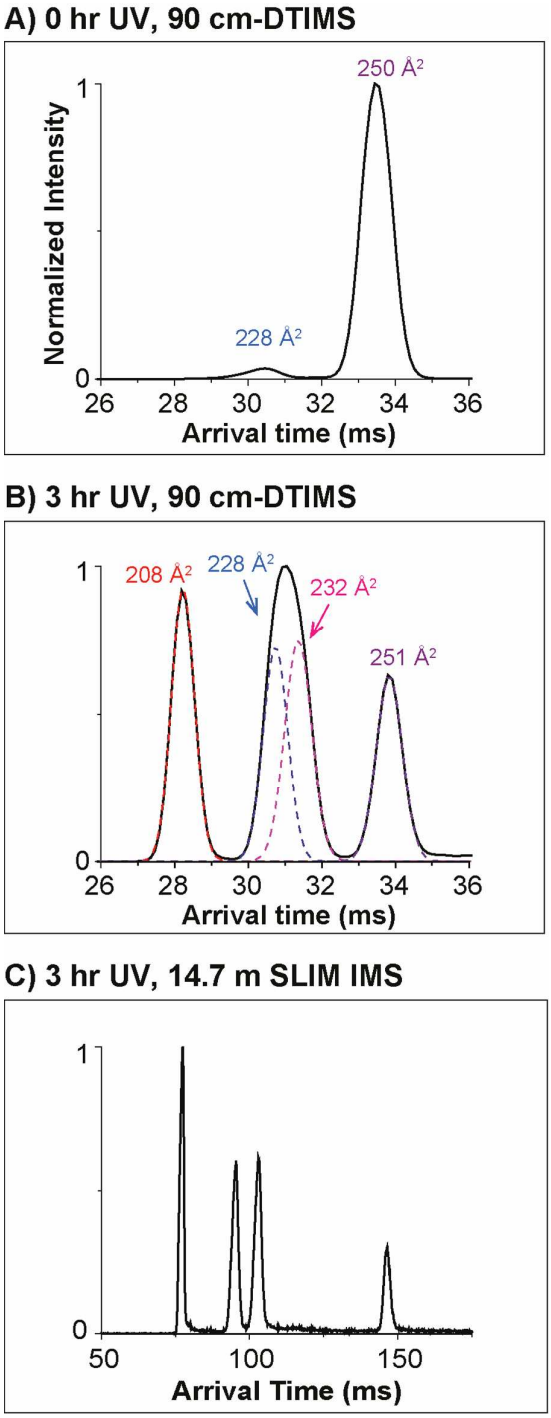


**Figure 2.** ATDs for the 3,5-diCQAs **A**) before UV irradiation and **B)** after 3 hr UV irradiation using the DTIMS-MS and **C**) the SLIM IMS-MS platforms. The dashed lines in **B**) represent the IMS peak shapes expected for single structures.

To better differentiate the 3,5-diCQA *cis*/*trans* isomers, SLIM IMS-MS measurements were performed for the conformers resulting from UV irradiation. As shown in Figure 2C



ACS Paragon Plus Environment

with only a 14.7 m SLIM IMS separation, the middle feature that was unresolved in Figure 2B is clearly separated into two features, confirming that there are four isomers for 3,5-diCQA after photoisomerization. To assign these *cis/trans* isomers, theoretical modelling was performed for each isomer allowing the calculation of theoretical CCS values (**Figure 3** and **Table 2**). By comparing the experimental and theoretical CCS values, the four ATD features were assigned (left to right) as: 3-*cis*,5-*cis,* 3-*trans*,5-*cis,* 3-*trans*,5-*cis* and 3-*trans*,5-*trans* (**Table 2**). The theoretical structures also revealed that the 3-*cis*,5-*cis* isomer has the most compact structure with the two caffeic acid (CA) groups/moeities collapsed toward each other, while the 3-*trans*,5-*trans* isomer was the most extended with the two CA groups widely open and extending in opposite directions. The 3-*cis*,5-*trans* and 3-*trans*,5-*cis* isomers both adapt a partially open conformation with one CA group collapsing toward the center and the other group extending to the side. The 3-*trans*,5-*cis* isomer however does have a slightly more open structure than the 3-*cis*,5-*trans* isomer resulting in a larger CCS value. Thus, the *cis* or *trans* orientation has an important impact on the molecule's conformation. Moreover, the intensity for 3-*cis*,5-*trans* isomer is similar to that of the 3-*trans*,5-*cis* isomer, indicating the chance of formation for these two isomers appears to be similar. To investigate this occurrence and the conversion pathways between the 3,5-diCQA isomers, we monitored the products formed after 2, 5, 10, 20 and 30 minutes of UV irradiation. Our analyses found that the *cis*,*cis* isomer only forms through 3-*cis*,5-*trans* and 3-*trans*,5-*cis* isomers not directly from the *trans*,*trans* isomer (see SI Figure S1). To estimate the reaction barriers associated with the transformation pathways from the 3-*trans*,5-*trans* isomer to the 3-*cis*,5-*cis* isomer, we determined the minimum energy paths using the "string method"[42] similar to Yoon et al.[43]. The reaction energies ($\Delta E$) along the minimum energy paths are depicted in Figure S2. The results illustrate that the conversion from 3-*trans*,5-*trans* to 3-*trans*,5-*cis* or 3-*cis*,5-*trans* is very high, explaining why diCQA exists as *trans*,*trans* until it is irradiated. They also



ACS Paragon Plus Environment

suggest that statistically, the 3-*trans*,5-*cis* isomer will form first, however, the energy barriers are similar and the photoisomerization process appears to result in the equivalent formation of 3-*trans*,5-*cis* and 3-*cis*,5-*trans*. Following the formation of the 3-*trans*,5-*cis* and 3-*cis*,5-*trans* isomers, the reaction barriers show that the 3-*cis*,5-*cis* isomer will preferentially arise from the 3-*cis*,5-*trans* isomer. Thus, by coupling the experimental IMS approach and theoretical calculations we were able to monitor the photoisomerization process and understand the conversions occurring between isomers.

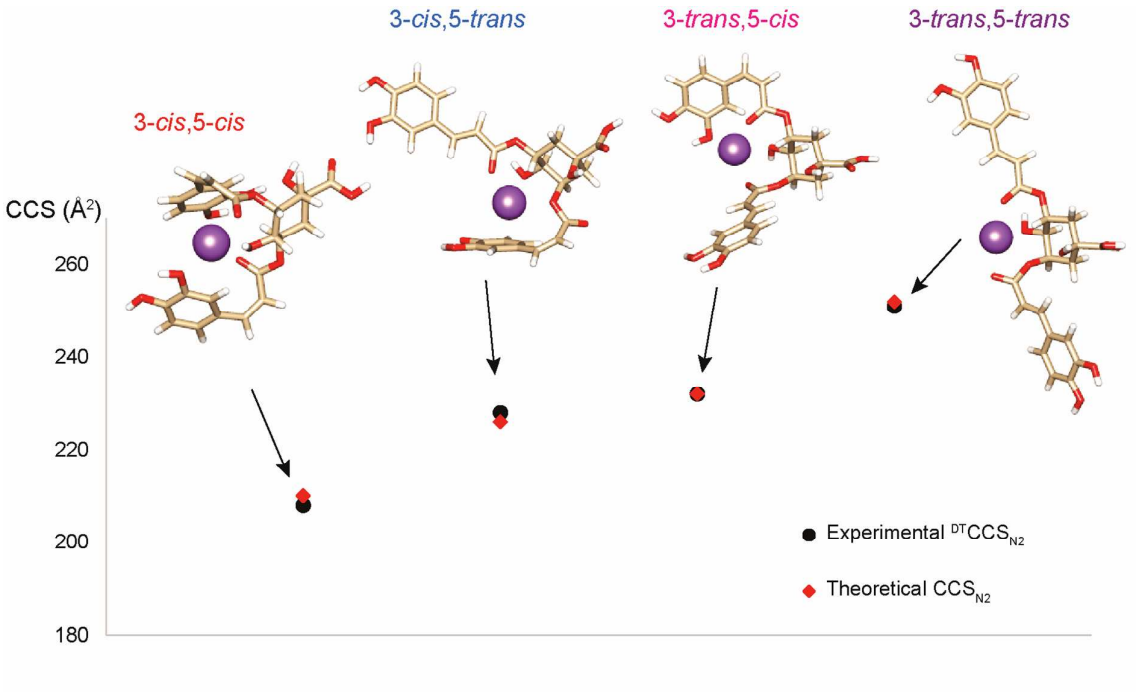


**Figure 3.** Theoretical modelling structures for the *cis*/*trans* photoisomerization products of 3,5-diCQA and their theoretical $CCS_{N2}$ values compared to the experimental $^{DT}CCS_{N2}$ values. The error associated with each measurement is noted in Table 2.



ACS Paragon Plus Environment

**Table 2. Theoretical and experimental CCS values (in Å$^2$) for each *cis/trans* 3,5-diCQA isomer.**

| 3,5-diCQA | Theoretical $CCS_{N2}$ (Å$^2$) | Theoretical CV (%) [a] | Experimental $^{DT}CCS_{N2}$ (Å$^2$) [b] | Experimental CV (%) |
|---|---|---|---|---|
| **3-*cis*,5-*cis*** | 210 | 0.2 | 208 | 0.3 |
| **3-*cis*,5-*trans*** | 226 | 0.2 | 228 | 0.1 |
| **3-*trans*,5-*cis*** | 232 | 0.1 | 232 | 0.4 |
| **3-*trans*,5-*trans*** | 252 | 0.2 | 251 | 0.3 |

[a] The theoretical CV is the deviation from the mean resulting from multiple calculations

[b] $^{DT}CCS_{N2}$ is the collision cross sections measured by DTIMS in nitrogen buffer gas

This manuscript tackles the difficult problem of identifying and quantifying *cis* and *trans* isomers of phytochemicals in natural product and plant extracts, which to date has been extremely challenging due to the vast structural diversity of the isomers present in the mixtures. Here IMS-based approaches were successfully utilized to separate complex diCQA isomers and identify the *cis*/*trans* isomers with the aid of theoretical modelling. The ultrahigh resolution SLIM IMS-MS technology enabled baseline separation of the isomers and was a powerful tool for analyzing the complex natural products and elucidating structure-activity relationships. Further, coupling the experiment IMS separations and theoretical calculations provided insight into isomeric conversions, which will be extremely important for drug discovery studies and optimizing specific bioactivities.

## METHODS

**Materials and Sample Preparations:** Authentic standards of *trans,trans*-dicaffeoylquinic acids (1,3-diCQA, 1,5-diCQA, 3,4-diCQA, 3,5-diCQA and 4,5-diCQA)

were purchased from Phytolab (Vestenbergsgreuth, Germany). Analytical grade methanol was purchased from Romil Ltd (Cambridge, UK). To obtain the cis isomers of the dicaffeoylquinic acids, a 1 mg/mL stock solution was prepared in 100% methanol. The samples were then irradiated using a UV lamp (Spectroline, USA) operating at 245 nm with an intensity of 390μW/cm$^2$. The lamp was not covered with any notch filter. The products of UV irradiation were analyzed by liquid chromatography-mass spectrometry[22] and no other species were observed other than those peaks corresponding to the 3,5-diCQA isomers (LC chromatograms shown in Figure S3). For the time-dependent photoisomerization study, the 3,5-diCQA was UV irradiated for 2, 5, 10, 20, 30, 60 and 180 minutes and the products were analysed by IMS-MS.

**DTIMS-MS:** The chemicals were analysed using an Agilent 6560 ion mobility-quadrupole time of flight mass spectrometry (IM-QTOF MS) platform [39-40]. Briefly, for ion mobility measurements, after electrospray ionization, ions were passed through the inlet glass capillary, focused by a high pressure ion funnel, and accumulated in a lower pressure ion funnel trap (IFT). Ions were then pulsed into the 90 cm-long IMS drift tube filled with ~ 4 torr of nitrogen gas, where they travel under the influence of a week electric field (10-20 V/cm). Ions exiting the drift tube were refocused by a rear ion funnel prior to QTOF MS detection and their arrival time ($t_A$) were recorded. The reduced mobility (the mobility scaled to standard temperature and pressure) can be determined from instrument parameters by plotting $t_A$ versus p/V [44]

$$t_A = \frac{L^2}{K_o}\left(\frac{273.15}{760\,T}\right)\left(\frac{p}{V}\right) + t_0$$

Here L is the drift length, V is the drift voltage, $t_0$ is the time ion spending outside of the drift cell, T is the drift gas temperature, and p is the drift gas pressure. The reduced mobility can be related to the collision cross sections of the analyte using kinetic theory [44]:

$$\Omega = \frac{3\,q}{16\,N}\left(\frac{2\,\pi}{\mu\,k_B\,T}\right)^{1/2}\frac{1}{K_0}$$

Here, q is the ion charge, N is the buffer gas number density at STP, μ is the reduced mass of the ion−Nitrogen collision, and $k_B$ is the Boltzmann constant. All the CCS values were measured using 7 stepped field voltages. Each measurement was performed in triplicate and the coefficient of variance (CV) was below 0.5% in all cases.

**SLIM-IMS-MS:** To achieve ultrahigh resolution IMS separation of the *cis/trans* isomers, the UV irradiated products of 3,5-diCQAs were also measured using a structures for lossless ion manipulations IMS-MS platform (SLIM IMS-MS). SLIM IMS uses traveling waves and a compact serpentine ion drift path for efficient ion selection, trapping and accumulations [33-38]. The SLIM IMS-MS platform has a 13 m long serpentine drift path and multipass capability, as recently described [38,45].

**Theoretical Calculations:** Molecular modeling was performed using NWChem (v6.6) [46], a high-performance computational chemistry software, similar to our previous studies [47-48]. Briefly, 2D structure files (.mol) were analyzed using the Marvin pKa plugin (Marvin 15.9.14, 2015, ChemAxon) for adduct site prediction [49]. Initial geometry relaxation was performed using the Merck molecular force field (MMFF94) [50] implemented in Avogadro (v1.1.1) [51]. Density functional theory (DFT) based *ab initio* molecular dynamics (AIMD) [52], as implemented in NWChem, was used to sample 100 conformers for each molecule [52]. AIMD calculations were each run for at least 10.2 ps, with conformers sampled every 101.6 fs. The AIMD temperature was maintained using a stochastic velocity rescaling thermostat [53]. This was followed by DFT-based frequency calculations for determining the Gibbs free energy of each conformer. The B3LYP exchange-correlation functional was used for all calculations [54-57] and Pople basis sets at the 3-21G level (a double-zeta split-valence potential basis set) [58-59] and 6-31G* level (a double-zeta valence potential basis set having a single



ACS Paragon Plus Environment

polarization function) [60-62], were used for the AIMD and DFT frequency calculations, respectively. All basis sets were obtained from the Environmental Molecular Sciences Laboratory (EMSL) Basis Set Exchange (bse.pnl.gov) [63-64]. NWChem output files were processed using custom-written Python scripts. Python (v2.7.10), with the NumPy package (v1.9.2) [65], was implemented using WinPython (v2.7.10.1, http://winpython.github.io), a free, open-source, and portable full-featured Python-based scientific environment. IPython (v3.2.0) [66], an enhanced Python shell, was used within the Scientific Python Development Environment (Spyder v2.3.5.2) for NWChem output data processing. Aided by supercomputers, our molecular modelling approach calculated CCS values with high accuracy, enabling the identification of the geometric isomers. The use of a first-principles theory (DFT) based AIMD approach enables consideration of the electronic structure of each isomer and its role in the conformer geometries. CCS values were calculated for all molecular conformers using the MOBCAL software, modified for the room temperature N2-based trajectory method [67-69]. The atom coordinates, radius, and charge distribution of the optimized geometry structures were used as input to the MOBCAL calculations. Final CCS values were obtained by a clustering approach using histogram distributions to determine the most abundant, low-energy, stable conformers. The scatter plots for the relative energy of 100 structures for each molecule as determined by ab initio calculations versus collision cross section as determined by MOBCAL. An example plot and frequency diagram are shown in Figure S4 for 3-*trans*,5-*cis* diCQA. NWChem was also used to calculate the minimum-energy paths using density functional theory (DFT) based zero temperature "string method". We employed 40 beads to represent each reaction path, for a total of 80 beads from 3-*trans*,5-*trans* diCQA to 3-*cis*,5-*cis* diCQA. The B3LYP exchange-correlation functional with the Pople basis set 3-21G was used for the string method with a stepsize of 0.1 and a maximum of 100 iterations.

## AUTHOR INFORMATION

**Corresponding authors**

*E-mail: erin.baker@pnnl.gov or emadala@uj.ac.za

**Notes**

The authors declare no competing financial interests.

## ACKNOWLEDGEMENTS

Portions of this research were supported by grants from the National Institute of Environmental Health Sciences of the NIH (R01 ES022190), National Institute of General Medical Sciences (P41 GM103493), and the Laboratory Directed Research and Development Program at Pacific Northwest National Laboratory for Global Forensic Chemical Exposure Assessment of the Environmental Exposome and Microbes in Transition (MinT) Initiative. This work was also partially funded by the South African National Research Foundation grant (TTK160604167903) awarded to NEM. This research utilized capabilities developed by the Pan-omics program (funded by the U.S. Department of Energy Office of Biological and Environmental Research Genome Sciences Program) and by the National Institute of Allergy and Infectious Diseases under grant U19AI106772. This work was performed in the W. R. Wiley Environmental Molecular Sciences Laboratory (EMSL), a DOE national scientific user facility at the Pacific Northwest National Laboratory (PNNL). The NWChem calculations were performed using the Cascade supercomputer at the EMSL. PNNL is operated by Battelle for the DOE under contract DE-AC05-76RL0 1830.

**Supporting Information Available:** Time-dependent study of the photoisomerization of 3,-5-diCQA by IMS-MS following UV irradiation; The minimum-energy paths from 3-*trans*,5-*trans* diCQA through 3-*trans*,5-*cis* diCQA and 3-*cis*,5-*trans* diCQA to 3-*cis*,5-*cis* diCQA using the ''string method" as implemented in NWChem; LC chromatograms for 3,5-diCQA before and after UV irradiation; An example scatter plot and cluster diagram for 3-trans,5-cis diCQA. The Supporting Information is available free of charge on the ACS Publications website.

## REFERENCES


1. Cho, A.-S.; Jeon, S.-M.; Kim, M.-J.; Yeo, J.; Seo, K.-I.; Choi, M.-S.; Lee, M.-K. Chlorogenic acid exhibits anti-obesity property and improves lipid metabolism in high-fat diet-induced-obese mice. *Amino Acids* **2010,** *48*, 937-943.
2. Urushisaki, T.; Takemura, T.; Tazawa, S.; Fukuoka, M.; Hosokawa-Muto, J.; Araki, Y.; Kuwata, K. Caffeoylquinic Acids Are Major Constituents with Potent Anti-Influenza Effects in Brazilian Green Propolis Water Extract. *Evidence-Based Complementary Altern. Med.* **2011,** *2011*, 1-7.
3. Ferlemi, A.-V.; Makri, O. E.; Mermigki, P. G.; Lamari, F. N.; Georgakopoulos, C. D. Quercetin glycosides and chlorogenic acid in highbush blueberry leaf decoction prevent cataractogenesis in vivo and in vitro: Investigation of the effect on calpains, antioxidant and metal chelating properties. *Exp. Eye Res.* **2016,** *145*, 258-268.
4. Clifford, M. N. Chlorogenic acids and other cinnamates – nature, occurrence, dietary burden, absorption and metabolism. *J. Sci. Food Agric.* **2000,** *80*, 1033-1043.
5. Jeng, T. L.; Lai, C. C.; Liao, T. C.; Lin, S. Y.; Sung, J. M. Effects of drying on caffeoylquinic acid derivative content and antioxidant capacity of sweet potato leaves. *J. Food Drug Anal.* **2015,** *23*, 701-708.
6. Könczöl, Á.; Béni, Z.; Sipos, M. M.; Rill, A.; Háda, V.; Hohmann, J.; Máthé, I.; Szántay Jr, C.; Keserű, G. M.; Balogh, G. T. Antioxidant activity-guided phytochemical investigation of Artemisia gmelinii Webb. ex Stechm.: Isolation and spectroscopic challenges of 3,5-O-dicaffeoyl (epi?) quinic acid and its ethyl ester. *J. Pharm. Biomed. Anal.* **2012,** *59*, 83-89.
7. Robinson, W. E.; Cordeiro, M.; Abdel-Malek, S.; Jia, Q.; Chow, S. A.; Reinecke, M. G.; Mitchell, W. M. Dicaffeoylquinic acid inhibitors of human immunodeficiency virus integrase: inhibition of the core catalytic domain of human immunodeficiency virus integrase. *Mol. Pharmacol.* **1996,** *50*, 846-855.
8. McDougall, B.; King, P. J.; Wu, B. W.; Hostomsky, Z.; Reinecke, M. G.; Robinson, W. E. Dicaffeoylquinic and Dicaffeoyltartaric Acids Are Selective Inhibitors of Human Immunodeficiency Virus Type 1 Integrase. *Antimicrob. Agents Chemother.* **1998,** *42*, 140-146.
9. Zhu, K.; Cordeiro, M. L.; Atienza, J.; Robinson, W. E.; Chow, S. A. Irreversible Inhibition of Human Immunodeficiency Virus Type 1 Integrase by Dicaffeoylquinic Acids. *J. Virol.* **1999,** *73*, 3309-3316.
10. Hong, S.; Joo, T.; Jhoo, J.-W. Antioxidant and anti-inflammatory activities of 3,5-dicaffeoylquinic acid isolated from Ligularia fischeri leaves. *Food Sci. Biotechnol.* **2015,** *24*, 257-263.
11. Abdel Motaal, A.; Ezzat, S. M.; Tadros, M. G.; El-Askary, H. I. In vivo anti-inflammatory activity of caffeoylquinic acid derivatives from Solidago virgaurea in rats. *Pharm. Biol.* **2016,** *54*, 2864-2870.

12. Arantes, A. A.; Fale, P. L.; Costa, L. C. B.; Pacheco, R.; Ascensao, L.; Serralheiro, M. L. Inhibition of HMG-CoA reductase activity and cholesterol permeation through Caco-2 cells by caffeoylquinic acids from Vernonia condensata leaves. *Rev. Bras. Farmacogn.-Brazilian Journal of Pharmacognosy* **2016,** *26*, 738-743.
13. Souza, A. H. P.; Corrêa, R. C. G.; Barros, L.; Calhelha, R. C.; Santos-Buelga, C.; Peralta, R. M.; Bracht, A.; Matsushita, M.; Ferreira, I. C. F. R. Phytochemicals and bioactive properties of Ilex paraguariensis: An in-vitro comparative study between the whole plant, leaves and stems. *Food Res. Int.* **2015,** *78*, 286-294.
14. Clifford, M. N.; Kirkpatrick, J.; Kuhnert, N.; Roozendaal, H.; Salgado, P. R. LC–MSn analysis of the cis isomers of chlorogenic acids. *Food Chem.* **2008,** *106*, 379-385.
15. Ramabulana, T.; Mavunda, R. D.; Steenkamp, P. A.; Piater, L. A.; Dubery, I. A.; Madala, N. E. Secondary metabolite perturbations in Phaseolus vulgaris leaves due to gamma radiation. *Plant Physiol. Biochem.* **2015,** *97*, 287-295.
16. Healy, E. F.; Sanders, J.; King, P. J.; Robinson Jr, W. E. A docking study of l-chicoric acid with HIV-1 integrase. *J. Mol. Graphics Modell.* **2009,** *27*, 584-589.
17. King, P. J.; Ma, G.; Miao, W.; Jia, Q.; McDougall, B. R.; Reinecke, M. G.; Cornell, C.; Kuan, J.; Kim, T. R.; Robinson, W. E. Structure−Activity Relationships: Analogues of the Dicaffeoylquinic and Dicaffeoyltartaric Acids as Potent Inhibitors of Human Immunodeficiency Virus Type 1 Integrase and Replication. *J. Med. Chem.* **1999,** *42*, 497-509.
18. Kyle, J. E.; Zhang, X.; Weitz, K. K.; Monroe, M. E.; Ibrahim, Y. M.; Moore, R. J.; Cha, J.; Sun, X.; Lovelace, E. S.; Wagoner, J., et al. Uncovering biologically significant lipid isomers with liquid chromatography, ion mobility spectrometry and mass spectrometry. *Analyst* **2016,** *141*, 1649-1659.
19. Gavino, V. C.; Gavino, G.; Leblanc, M.-J.; Tuchweber, B. An Isomeric Mixture of Conjugated Linoleic Acids But Not Pure cis-9,trans-11-Octadecadienoic Acid Affects Body Weight Gain and Plasma Lipids in Hamsters. *J. Nutr.* **2000,** *130*, 27-29.
20. Kawamura, S.; Unno, Y.; List, A.; Mizuno, A.; Tanaka, M.; Sasaki, T.; Arisawa, M.; Asai, A.; Groll, M.; Shuto, S. Potent Proteasome Inhibitors Derived from the Unnatural cis-Cyclopropane Isomer of Belactosin A: Synthesis, Biological Activity, and Mode of Action. *J. Med. Chem.* **2013,** *56*, 3689-3700.
21. Mncwangi, N. P.; Viljoen, A. M.; Zhao, J.; Vermaak, I.; Chen, W.; Khan, I. What the devil is in your phytomedicine? Exploring species substitution in Harpagophytum through chemometric modeling of 1H-NMR and UHPLC-MS datasets. *Phytochemistry* **2014,** *106*, 104-115.
22. Clifford, M. N.; Johnston, K. L.; Knight, S.; Kuhnert, N. Hierarchical Scheme for LC-MSn Identification of Chlorogenic Acids. *J. Agric. Food. Chem.* **2003,** *51*, 2900-2911.
23. Clifford, M. N.; Knight, S.; Kuhnert, N. Discriminating between the Six Isomers of Dicaffeoylquinic Acid by LC-MSn. *J. Agric. Food. Chem.* **2005,** *53*, 3821-3832.
24. Makola, M. M.; Steenkamp, P. A.; Dubery, I. A.; Kabanda, M. M.; Madala, N. E. Preferential alkali metal adduct formation by cis geometrical isomers of dicaffeoylquinic acids allows for efficient discrimination from their trans isomers during ultra-high-performance liquid chromatography/quadrupole time-of-flight mass spectrometry. *Rapid Commun. Mass Spectrom.* **2016,** *30*, 1011-1018.
25. Bohrer, B. C.; Merenbloom, S. I.; Koeniger, S. L.; Hilderbrand, A. E.; Clemmer, D. E. Biomolecule Analysis by Ion Mobility Spectrometry. *Annu. Rev. Anal. Chem.* **2008,** *1*, 293-327.
26. Lanucara, F.; Holman, S. W.; Gray, C. J.; Eyers, C. E. The power of ion mobility-mass spectrometry for structural characterization and the study of conformational dynamics. *Nat. Chem.* **2014,** *6*, 281-294.
27. Lapthorn, C.; Pullen, F.; Chowdhry, B. Z. Ion mobility spectrometry-mass spectrometry (IMS-MS) of small molecules: Separating and assigning structures to ions. *Mass Spectrom. Rev.* **2013,** *32*, 43-71.
28. Baker, E. S.; Hong, J. W.; Gidden, J.; Bartholomew, G. P.; Bazan, G. C.; Bowers, M. T. Diastereomer Assignment of an Olefin-Linked Bis-paracyclophane by Ion Mobility Mass Spectrometry. *J. Am. Chem. Soc.* **2004,** *126*, 6255-6257.

29. Adamson, B. D.; Coughlan, N. J. A.; Markworth, P. B.; Continetti, R. E.; Bieske, E. J. An ion mobility mass spectrometer for investigating photoisomerization and photodissociation of molecular ions. *Rev. Sci. Instrum.* **2014,** *85*, 123109-112317.
30. Czerwinska, I.; Kulesza, A.; Choi, C.; Chirot, F.; Simon, A.-L.; Far, J.; Kune, C.; de Pauw, E.; Dugourd, P. Supramolecular influence on cis-trans isomerization probed by ion mobility spectrometry. *PCCP* **2016,** *18*, 32331-32336.
31. Xie, C.; Yu, K.; Zhong, D.; Yuan, T.; Ye, F.; Jarrell, J. A.; Millar, A.; Chen, X. Investigation of Isomeric Transformations of Chlorogenic Acid in Buffers and Biological Matrixes by Ultraperformance Liquid Chromatography Coupled with Hybrid Quadrupole/Ion Mobility/Orthogonal Acceleration Time-of-Flight Mass Spectrometry. *J. Agric. Food. Chem.* **2011,** *59*, 11078-11087.
32. Kuhnert, N.; Yassin, G. H.; Jaiswal, R.; Matei, M. F.; Grün, C. H. Differentiation of prototropic ions in regioisomeric caffeoyl quinic acids by electrospray ion mobility mass spectrometry. *Rapid Commun. Mass Spectrom.* **2015,** *29*, 675-680.
33. Zhang, X.; Garimella, S. V. B.; Prost, S. A.; Webb, I. K.; Chen, T.-C.; Tang, K.; Tolmachev, A. V.; Norheim, R. V.; Baker, E. S.; Anderson, G. A., et al. Ion Trapping, Storage, and Ejection in Structures for Lossless Ion Manipulations. *Anal. Chem.* **2015,** *87*, 6010-6016.
34. Chen, T.-C.; Ibrahim, Y. M.; Webb, I. K.; Garimella, S. V. B.; Zhang, X.; Hamid, A. M.; Deng, L.; Karnesky, W. E.; Prost, S. A.; Sandoval, J. A., et al. Mobility-Selected Ion Trapping and Enrichment Using Structures for Lossless Ion Manipulations. *Anal. Chem.* **2016,** *88*, 1728-1733.
35. Hamid, A. M.; Garimella, S. V.; Ibrahim, Y. M.; Deng, L.; Zheng, X.; Webb, I. K.; Anderson, G. A.; Prost, S. A.; Norheim, R. V.; Tolmachev, A. V., et al. Achieving High Resolution Ion Mobility Separations Using Traveling Waves in Compact Multiturn Structures for Lossless Ion Manipulations. *Anal. Chem.* **2016,** *88*, 8949-8956.
36. Deng, L.; Ibrahim, Y. M.; Hamid, A. M.; Garimella, S. V. B.; Webb, I. K.; Zheng, X.; Prost, S. A.; Sandoval, J. A.; Norheim, R. V.; Anderson, G. A., et al. Ultra-High Resolution Ion Mobility Separations Utilizing Traveling Waves in a 13 m Serpentine Path Length Structures for Lossless Ion Manipulations Module. *Anal. Chem.* **2016,** *88*, 8957-8964.
37. Deng, L.; Ibrahim, Y. M.; Garimella, S. V. B.; Webb, I. K.; Hamid, A. M.; Norheim, R. V.; Prost, S. A.; Sandoval, J. A.; Baker, E. S.; Smith, R. D. Greatly Increasing Trapped Ion Populations for Mobility Separations Using Traveling Waves in Structures for Lossless Ion Manipulations. *Anal. Chem.* **2016,** *88*, 10143-10150.
38. Deng, L.; Ibrahim, Y. M.; Baker, E. S.; Aly, N. A.; Hamid, A. M.; Zhang, X.; Zheng, X.; Garimella, S. V. B.; Webb, I. K.; Prost, S. A., et al. Ion Mobility Separations of Isomers based upon Long Path Length Structures for Lossless Ion Manipulations Combined with Mass Spectrometry. *ChemistrySelect* **2016,** *1*, 2396-2399.
39. May, J. C.; Goodwin, C. R.; Lareau, N. M.; Leaptrot, K. L.; Morris, C. B.; Kurulugama, R. T.; Mordehai, A.; Klein, C.; Barry, W.; Darland, E., et al. Conformational Ordering of Biomolecules in the Gas Phase: Nitrogen Collision Cross Sections Measured on a Prototype High Resolution Drift Tube Ion Mobility-Mass Spectrometer. *Anal. Chem.* **2014,** *86*, 2107-2116.
40. Ibrahim, Y. M.; Baker, E. S.; Danielson, W. F., 3rd; Norheim, R. V.; Prior, D. C.; Anderson, G. A.; Belov, M. E.; Smith, R. D. Development of a New Ion Mobility (Quadrupole) Time-of-Flight Mass Spectrometer. *Int J Mass Spectrom* **2015,** *377*, 655-662.
41. Makola, M. M.; Dubery, I. A.; Koorsen, G.; Steenkamp, P. A.; Kabanda, M. M.; du Preez, L. L.; Madala, N. E. The Effect of Geometrical Isomerism of 3,5-Dicaffeoylquinic Acid on Its Binding Affinity to HIV-Integrase Enzyme: A Molecular Docking Study. *Evidence-Based Complementary Altern. Med.* **2016,** *2016*, 1-9.
42. E, W.; Ren, W.; Vanden-Eijnden, E. String method for the study of rare events. *Phys. Rev. B* **2002,** *66*, 052301-052304.
43. Yoon, M.; Han, S.; Kim, G.; Lee, S. B.; Berber, S.; Osawa, E.; Ihm, J.; Terrones, M.; Banhart, F.; Charlier, J.-C., et al. Zipper Mechanism of Nanotube Fusion: Theory and Experiment. *Phys. Rev. Lett.* **2004,** *92*, 075504-075507.
44. Mason, E. A.; McDaniel, E. W. Kinetic Theory of Mobility and Diffusion: Sections 5.1 – 5.2. In *Transport Properties of Ions in Gases*, Wiley-VCH Verlag GmbH & Co. KGaA: 2005; pp 137-193.

45. Deng, L.; Ibrahim, Y. M.; Hamid, A. M.; Garimella, S. V.; Webb, I. K.; Zheng, X.; Prost, S. A.; Sandoval, J. A.; Norheim, R. V.; Anderson, G. A., et al. Ultra-High Resolution Ion Mobility Separations Utilizing Traveling Waves in a 13 m Serpentine Path Length Structures for Lossless Ion Manipulations Module. *Anal. Chem.* **2016,** *88*, 8957-8964.
46. Valiev, M.; Bylaska, E. J.; Govind, N.; Kowalski, K.; Straatsma, T. P.; Van Dam, H. J. J.; Wang, D.; Nieplocha, J.; Apra, E.; Windus, T. L., et al. NWChem: A comprehensive and scalable open-source solution for large scale molecular simulations. *Comput. Phys. Commun.* **2010,** *181*, 1477-1489.
47. Graham, T. R.; Renslow, R.; Goyind, N.; Saunders, S. R. Precursor Ion-Ion Aggregation in the Brust-Schiffrin Synthesis of Alkanethiol Nanoparticles. *J. Phys. Chem. C* **2016,** *120*, 19837-19847.
48. Zheng, X.; Zhang, X.; Schocker, N. S.; Renslow, R. S.; Orton, D. J.; Khamsi, J.; Ashmus, R. A.; Almeida, I. C.; Tang, K.; Costello, C. E., et al. Enhancing glycan isomer separations with metal ions and positive and negative polarity ion mobility spectrometry-mass spectrometry analyses. *Anal. Bioanal. Chem.* **2016**, 1-10.
49. Csizmadia, J. S. a. F. In *A method for calculating the pKa values of small and large molecules*, American Chemical Society Spring meeting, March 25-29th, 2007.
50. Halgren, T. A. Merck molecular force field. I. Basis, form, scope, parameterization, and performance of MMFF94. *J. Comput. Chem.* **1996,** *17*, 490-519.
51. Hanwell, M. D.; Curtis, D. E.; Lonie, D. C.; Vandermeersch, T.; Zurek, E.; Hutchison, G. R. Avogadro: an advanced semantic chemical editor, visualization, and analysis platform. *J. Cheminf.* **2012,** *4*, 1-17.
52. Fischer, S. A.; Ueltschi, T. W.; El-Khoury, P. Z.; Mifflin, A. L.; Hess, W. P.; Wang, H.-F.; Cramer, C. J.; Govind, N. Infrared and Raman Spectroscopy from Ab Initio Molecular Dynamics and Static Normal Mode Analysis: The C–H Region of DMSO as a Case Study. *J. Phys. Chem. B* **2016,** *120*, 1429-1436.
53. Bussi, G.; Donadio, D.; Parrinello, M. Canonical sampling through velocity rescaling. *J. Chem. Phys.* **2007,** *126*, 014101-014107.
54. Becke, A. D. Density-functional thermochemistry. III. The role of exact exchange. *J. Chem. Phys.* **1993,** *98*, 5648-5652.
55. Lee, C.; Yang, W.; Parr, R. G. Development of the Colle-Salvetti correlation-energy formula into a functional of the electron density. *Phys. Rev. B* **1988,** *37*, 785-789.
56. Vosko, S. H.; Wilk, L.; Nusair, M. Accurate spin-dependent electron liquid correlation energies for local spin density calculations: a critical analysis. *Can. J. Phys.* **1980,** *58*, 1200-1211.
57. Stephens, P. J.; Devlin, F. J.; Chabalowski, C. F.; Frisch, M. J. Ab Initio Calculation of Vibrational Absorption and Circular Dichroism Spectra Using Density Functional Force Fields. *J. Phys. Chem.* **1994,** *98*, 11623-11627.
58. Binkley, J. S.; Pople, J. A.; Hehre, W. J. Self-Consistent Molecular-Orbital Methods .21. Small Split-Valence Basis-Sets for 1st-Row Elements. *J. Am. Chem. Soc.* **1980,** *102*, 939-947.
59. Gordon, M. S.; Binkley, J. S.; Pople, J. A.; Pietro, W. J.; Hehre, W. J. Self-Consistent Molecular-Orbital Methods .22. Small Split-Valence Basis-Sets for 2nd-Row Elements. *J. Am. Chem. Soc.* **1982,** *104*, 2797-2803.
60. Francl, M. M.; Pietro, W. J.; Hehre, W. J.; Binkley, J. S.; Gordon, M. S.; DeFrees, D. J.; Pople, J. A. Self-consistent molecular orbital methods. XXIII. A polarization-type basis set for second-row elements. *J. Chem. Phys.* **1982,** *77*, 3654-3665.
61. Hariharan, P. C.; Pople, J. A. The influence of polarization functions on molecular orbital hydrogenation energies. *Theor. Chim. Acta* **1973,** *28*, 213-222.
62. Rassolov, V. A.; Ratner, M. A.; Pople, J. A.; Redfern, P. C.; Curtiss, L. A. 6-31G* basis set for third-row atoms. *J. Comput. Chem.* **2001,** *22*, 976-984.
63. Feller, D. The role of databases in support of computational chemistry calculations. *J. Comput. Chem.* **1996,** *17*, 1571-1586.
64. Schuchardt, K. L.; Didier, B. T.; Elsethagen, T.; Sun, L. S.; Gurumoorthi, V.; Chase, J.; Li, J.; Windus, T. L. Basis set exchange: A community database for computational sciences. *J. Chem. Inf. Model.* **2007,** *47*, 1045-1052.

65. van der Walt, S.; Colbert, S. C.; Varoquaux, G. The NumPy Array: A Structure for Efficient Numerical Computation. *Comput. Sci. Eng.* **2011,** *13*, 22-30.
66. Perez, F.; Granger, B. E. IPython: A system for interactive scientific computing. *Comput. Sci. Eng.* **2007,** *9*, 21-29.
67. Campuzano, I.; Bush, M. F.; Robinson, C. V.; Beaumont, C.; Richardson, K.; Kim, H.; Kim, H. I. Structural Characterization of Drug-like Compounds by Ion Mobility Mass Spectrometry: Comparison of Theoretical and Experimentally Derived Nitrogen Collision Cross Sections. *Anal. Chem.* **2012,** *84*, 1026-1033.
68. Mesleh, M. F.; Hunter, J. M.; Shvartsburg, A. A.; Schatz, G. C.; Jarrold, M. F. Structural information from ion mobility measurements: Effects of the long-range potential. *J. Phys. Chem.* **1996,** *100*, 16082-16086.
69. Shvartsburg, A. A.; Jarrold, M. F. An exact hard-spheres scattering model for the mobilities of polyatomic ions. *Chem. Phys. Lett.* **1996,** *261*, 86-91.

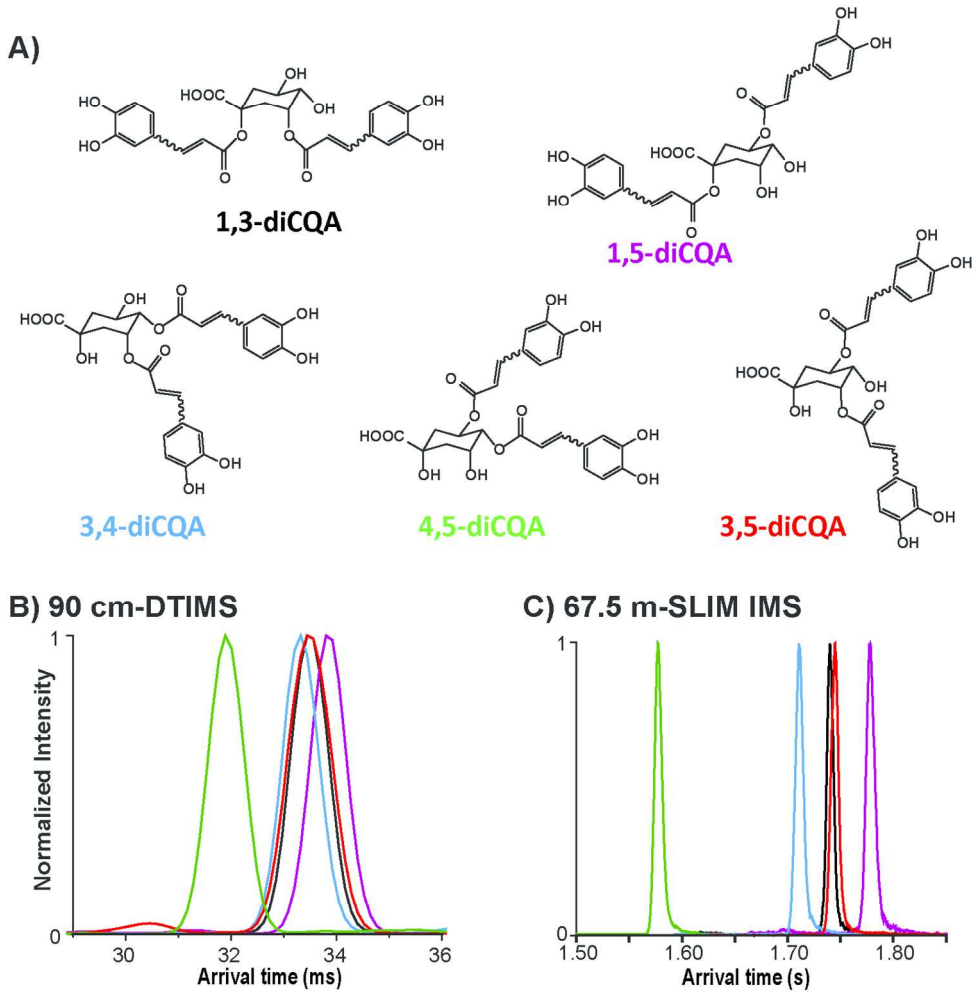


Figure 1. IMS characterization of the dicaffeoylquinic acid positional isomers 1,3-diCQA, 1,5-diCQA, 3,4-diCQA, 3,5-diCQA and 4,5-diCQA. A) The chemical structures of each isomer and arrival time distributions (ATDs) using a B) DTIMS platform and C) ultrahigh resolution SLIM IMS.

140x139mm (300 x 300 DPI)

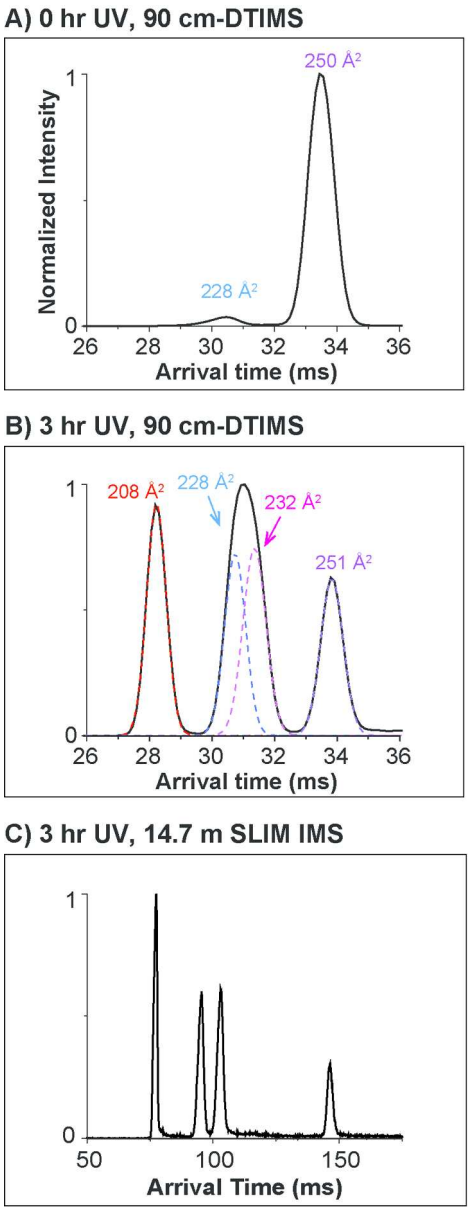


ATDs for the 3,5-diCQAs A) before UV irradiation and B) after 3 hr UV irradiation using the DTIMS-MS and C) the SLIM IMS-MS platforms. The dashed lines in B) represent the IMS peak shapes expected for single structures.

76x198mm (300 x 300 DPI)

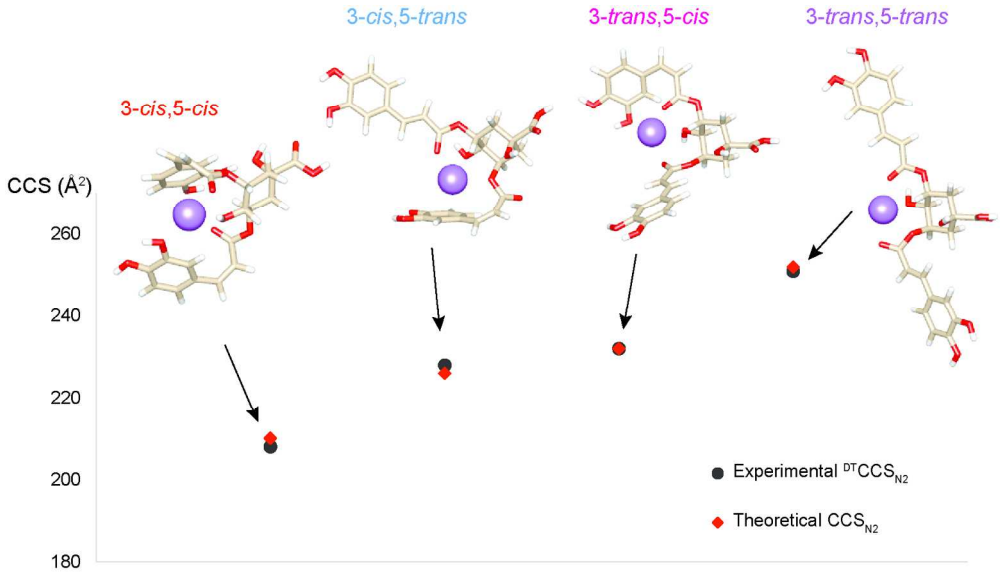


Theoretical modelling structures for the cis/trans photoisomerization products of 3,5-diCQA and their theoretical CCSN2 values compared to the experimental DTCCSN2 values. The error associated with each measurement is noted in Table 2.

161x97mm (300 x 300 DPI)

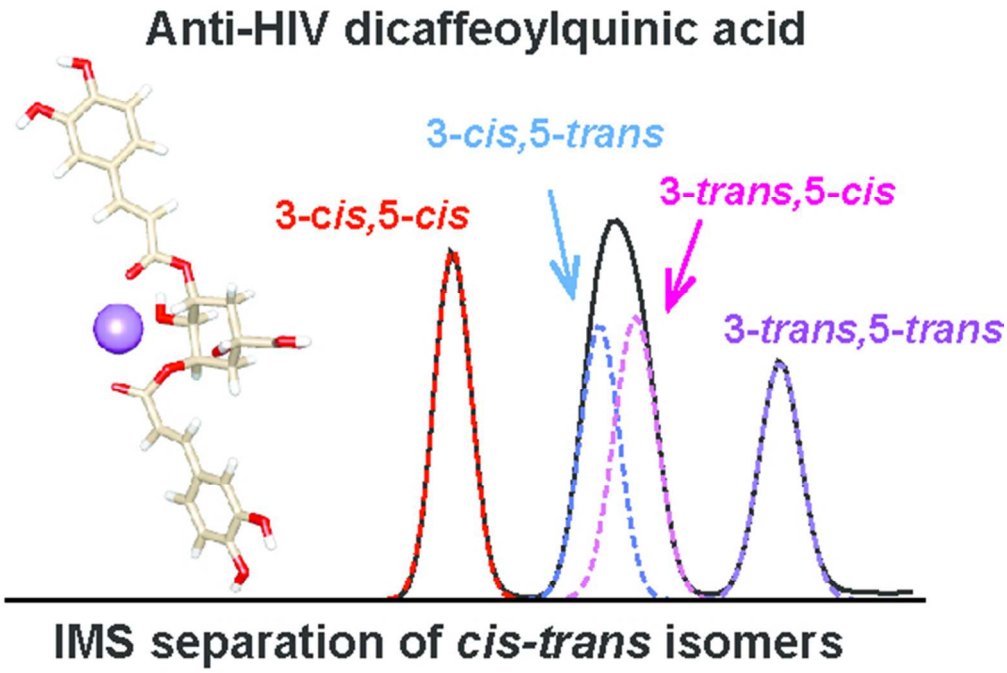


IMS separation of cis-trans isomers of dicaffeoylquinic acid.

52x35mm (300 x 300 DPI)